# Proton Nuclear Magnetic Resonance Investigation of the Conformation and Dynamics in the Synthetic Deoxyribonucleic Acid Decamers d(ATATCGATAT) and d(ATATGCATAT)†

Juli Feigon,‡ William A. Denny,§ Werner Leupin,⊥ and David R. Kearns*

ABSTRACT: A variety of one-dimensional proton NMR methods have been used to investigate the properties of two synthetic DNA decamers, d(ATATCGATAT) and d(ATATGCATAT). These results, in conjunction with the results of two-dimensional NMR experiments, permit complete assignment of the base proton resonances. Low-field resonances were assigned by sequential "melting" of the A·T base pairs and by comparison of the spectra of the two decamers. Below 20 °C spin–lattice relaxation is dominated by through-space dipolar interactions. A substantial isotope effect on the G imino proton relaxation is observed in 75% $D_2O$, confirming the importance of the exchangeable amino protons in the relaxation process. A somewhat smaller isotope effect is observed on the T imino proton relaxation. At elevated temperatures spin–lattice relaxation of the imino protons is due to proton exchange with solvent. Apparent activation energies for exchange vary from 36 kcal/base pair for base pairs (3,8) to 64 kcal/mol for the most interior base pairs (5,6), indicating that disruption of part, or all, of the double helix contributes significantly to the exchange of the imino protons in these decamers. By contrast, single base pair opening events are the major low-temperature pathways for exchange from A·T and G·C base pairs in the more stable higher molecular weight DNA examined in other studies. The temperature dependence of the chemical shifts and line widths of certain aromatic resonances indicates that the interconversion between the helix and coil states is not in fast exchange below the melting temperature, $T_m$. Within experimental error, no differential melting of base pairs was found in either molecule, and both exhibited melting points $T_m$ = 50–52 °C. Spin–spin and spin–lattice relaxation rates of the nonexchangeable protons (TH6, AH8, and AH2) are consistent with values calculated by using an isotropic rotor model with a rotational correlation time of 6 ns and interproton distances appropriate for B-family DNA. The faster decay of AH8 compared with GH8 is attributed to an interaction between the thymine methyl protons and the AH8 protons in adjacent adenines (5′ApT3′). The base protons (AH8, GH8, and TH6) appear to be located close (1.9–2.3 Å) to sugar H2′,2″ protons. A cross-strand AH2–AH2 interaction (interproton distance of 2.8 ± 0.2 Å) is manifested in terms of a larger $R_2$ value for bases $A_3$ and $A_9$ compared to $A_1$ and $A_7$. The spin–spin couplings ($J_{1'2'} + J_{1'2''}$) for the H1′ sugar resonances indicate that most sugar groups in the molecule are in S conformation, consistent with a B-family DNA conformation.

Recent studies have demonstrated that DNA molecules can adopt a much wider range of conformational states than had been previously suspected (Wang et al., 1979; Drew et al., 1980) and that there are interesting conformational transitions in DNA molecules which are sensitive to base modification and environment (Behe & Felsenfeld, 1981) and to the topological state of the DNA (Klysik et al., 1981; Peck et al., 1982; Wartell et al., 1982). The unexpected discovery of Z-DNA by Wang et al. (1979) has clearly demonstrated that a DNA with a $d(CG)_n$ sequence is capable of adopting a left-handed conformation. Supercoiled DNAs have been demonstrated to have unexpected NMR properties (Bendel et al., 1982). Although these and other studies greatly expand our understanding of the physical properties of DNA, they raise new questions about the structural and dynamic properties of DNA in solution which have not, or could not, be answered by using previous conventional spectroscopic approaches. However, it now appears that pulsed nuclear magnetic resonance (NMR) techniques can be used to systematically explore both structural and dynamic properties of DNA at a level of detail that was previously not possible.

Most previous proton NMR studies of DNA have concentrated on measurements of chemical shifts and splittings of resonances, but unfortunately, the experimentally observed chemical shifts contain a large number of contributions that are too difficult to calculate theoretically and to relate to DNA structure (Kearns, 1977, 1983). NMR relaxation rates (phenomena), on the other hand, can be directly related to the structural and dynamic properties of the DNA. In several earlier studies we have reported proton spin–lattice and spin–spin relaxation studies on the exchangeable and nonexchangeable protons of random sequence double-helical DNA (Early & Kearns, 1979; Early et al., 1980) and in poly(dA-dT) (Kearns et al., 1981). We also carried out extensive studies of the relaxation behavior of protons in a 12 base pair DNA restriction fragment (Early et al., 1980, 1980a,b), but interpretation of these measurements was limited by problems in assigning the spectra.

In this paper we present the first part of an investigation of the conformational and dynamic properties of two synthetic self-complementary DNA decamers, d(ATATCGATAT) and d(ATATGCATAT). When a combination of techniques is used, resonances from all of the base protons and some of the sugar protons can be assigned to specific base pairs in the

† From the Department of Chemistry, University of California—San Diego, La Jolla, California 92093. *Received April 26, 1983.* This work was supported by the American Cancer Society (Grant CH32 to D.R.K.) and the National Science Foundation (Grant PCM-7911571 to D.R.K.). UCSD Chemistry Department NMR Center was supported in part by funds from the National Science Foundation. W.L. was supported by a grant from the Swiss National Science Foundation. Part of this work was from Feigon (1982).

‡ Present address: Biology Department, Massachusetts Institute of Technology, Cambridge, MA 02139.

§ Present address: Cancer Chemotherapy Research Laboratory, University of Auckland, School of Medicine, Private Bag, Auckland, New Zealand.

⊥ Present address: Institut fur Molecularbiologie und Biophysik, Eidgenossische Technische Hochschule, CH-8093 Zurich, Switzerland.

0006-2960/83/0422-5930$01.50/0 

molecule. Moreover, because the decamers are relatively small (34 Å × 24 Å), they have relatively short rotational correlation times and, to a good first approximation, tumble in solution like an isotropic rotor. Both features simplify the theoretical analysis of the relaxation rates (Wöessner, 1962). In this paper we are concerned with the assignment of spectra, determination of the sugar coupling constants, and measurement of the spin–lattice and spin–spin relaxation rates for the exchangeable imino and nonexchangeable aromatic protons. From measurements carried out over a range of temperatures, we obtain information on the mechanisms of relaxation, the dynamics of base pair opening, and details of thermal denaturation in these two molecules. Modulations of Hahn spin echoes and resolution-enhanced spectra are used to extract information about sugar coupling constants and, hence, sugar conformations. The effect of deuteration of the exchangeable amino protons on the relaxation of the T and G imino protons has been used to probe dipolar contributions to the relaxation of the imino protons. Relaxation rates are used to make preliminary deductions about certain structural features in the molecule. This work was completed in 1982 (Feigon), and a preliminary account was presented elsewhere (Feigon et al., 1982).

The results of this one-dimensional NMR study and a two-dimensional NMR study of d(ATATCGATAT) described in the following paper (Feigon et al., 1983) provide the qualitative information necessary for more quantitative investigations of the structures of these molecules in solution and their interactions with other ligands such as metal ions and drugs.

## Materials and Methods

*Materials.* The two DNA decamers were prepared by using a modified phosphotriester method in liquid phase as described elsewhere (Denny et al., 1982b). The sodium form of the decamers were ethanol precipitated, dried, and redissolved, after weighing, in 10 mM sodium phosphate, pH 7.0, and 0.1 M NaCl to concentrations of ~20 mg/mL (~3 mM in duplex). Unless otherwise noted, all samples were run in Wilmad 508 cp microcells containing ~120 μL of solution. For spectra in $D_2O$, the water samples were dried down in the NMR tube under a stream of $N_2$ at least twice and redissolved with 99.996% $D_2O$ (Stohler Isotopes).

*Methods.* Spectra of the low-field resonances of the DNA decamers in water were taken in the correlation mode on a Varian 300 MHz spectrometer, and temperature was controlled to ±1 °C by the Varian temperature controller. All spectra and relaxation measurements in $D_2O$ were taken on the UCSD Chemistry Department 360 MHz NMR spectrometer (Wright et al., 1981). Chemical shifts (ppm) were determined relative to the chemical shift of water (or the residual HDO peak), which had been referenced to sodium 4,4-dimethyl-4-silapentane-1-sulfonate (DSS) as a function of temperature.

## Results

Figure 1A shows the sequences of the two decamers along with the numbering system used. The two decamers will sometimes be referred to as "CG" or "GC" where they are distinguished from each other by the difference in their sequence when reading from the 5′ to the 3′ end. The structures of the base pairs and the deoxyribose sugar are shown in Figure 1B, illustrating the protons of interest.

(*A*) *Imino Proton Resonance: Assignments and Temperature Dependence.* Figure 2A shows the temperature dependence of the low-field spectra of the two decamers d-

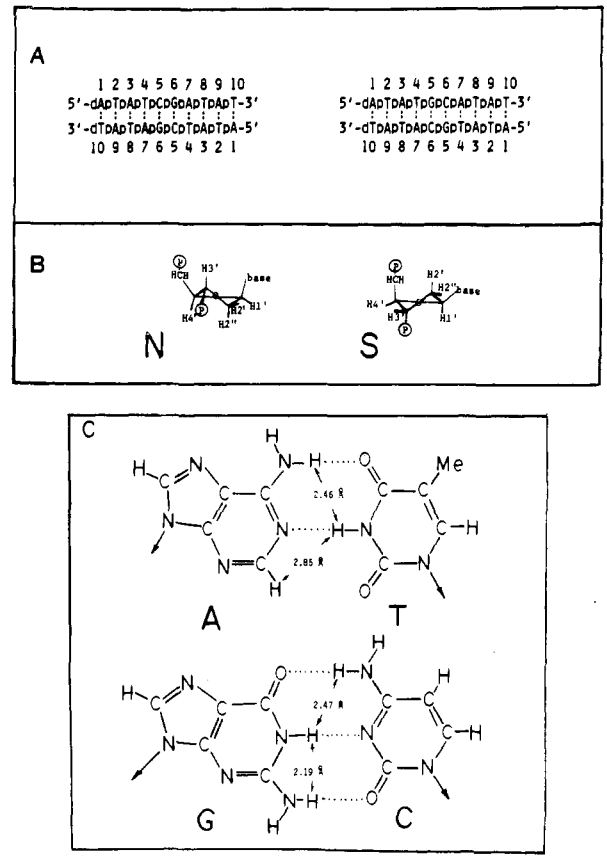


FIGURE 1: (A) Sequences of the two decamers are shown with the numbering sequence used. Neither the 5′ nor the 3′ end has a terminal phosphate. (B) Perspective views of the N and S sugar conformations. (C) The standard A·T and G·C base pairs are shown with interproton distances.

(ATATCGATAT) and d(ATATGCATAT). Because of symmetry [base pairs (1,10), (2,9), (3,8), (4,7), and (5,6) are equivalent pairs] a maximum of five downfield resonances of two protons each are expected. In this context, future reference to one resonance will imply that it arises from two equivalent protons.

In the low-field spectra, the single resonance at about 12.5 ppm can clearly be assigned to the G·C base pair imino protons in each molecule, while the collection of resonances at lower field is due to the imino protons of the A·T base pairs (Kearns, 1977). Although ring current calculations (Arter & Schmidt, 1976) predict that the G·C imino protons in both molecules should be ring current shifted upfield by almost exactly the same amount (1.27 ppm for "GC" and 1.28 ppm for "CG"), the G·C imino protons in d(ATATGCATAT) actually resonate ~0.1 ppm upfield from those in d(ATATCGATAT).

At 24 °C, only two sharp A·T imino resonances from each molecule are present. The imino protons from the remaining A·T base pairs exchange rapidly with $H_2O$ at this temperature on the NMR time scale and thus appear as very broad peaks beneath the two A·T resonances [base pairs (2,9)] and on the low-field side of the G·C resonance (terminal base pairs) (Patel & Hilbers, 1975). Because of their sequences, these molecules are expected to open first from the ends of the helix. Early (i.e., low-temperature) broadening and disappearance of the imino proton resonances from the terminal and next-to-terminal base pairs in oligonucleotides have been previously observed (Patel & Hilbers, 1975; Kan et al., 1975) and attributed to fraying of the ends. Therefore, by following the successive broadening and shifting of the low-field A·T imino resonances with temperature, all of the low-field resonances can be as-

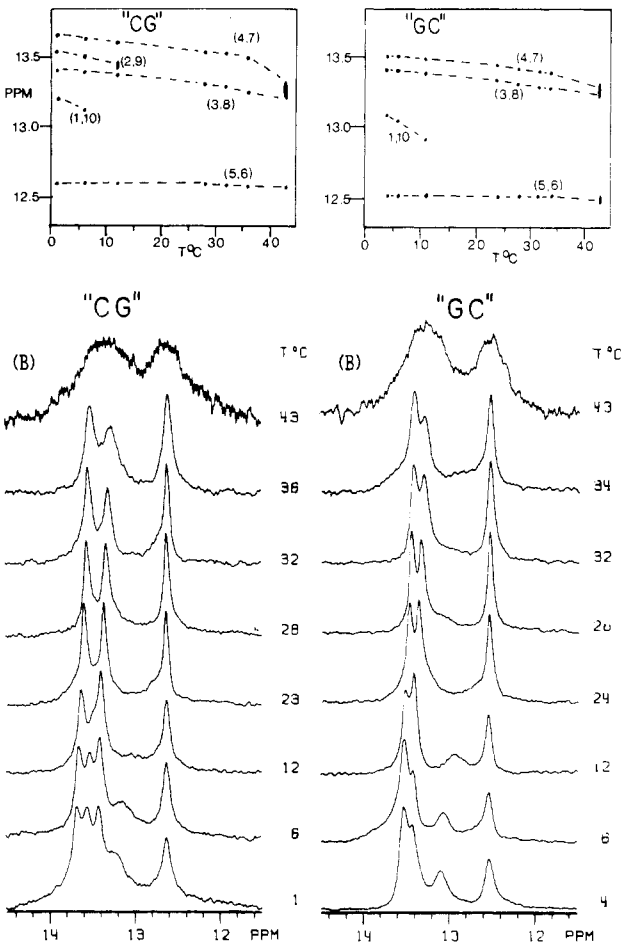


FIGURE 2: Temperature dependence of the 300-MHz low-field spectra (imino resonances) of d(ATATCGATAT) (left) and d(ATATGCATAT) (right) at 300 MHz. (Top) Chemical shifts are plotted as a function of temperature. Note that assignments of the resonances are also indicated. (Bottom) Low-field spectra are shown at several temperatures; 2000–4000 transients were collected with a sweep time of 0.5 s, a predelay of 0.50 ms, a 1500 Hz sweep width, and 2 Hz line broadening. Spectra are plotted to have the same maximum peak height, but relative intensities can be estimated by a comparison of the S/N of the spectra. Note that the absolute intensity of the resonances from the G·C imino protons (~12.5 ppm) should be invariant over most of the temperature range studied.

signed in both decamers. These assignments are summarized in Figure 2 (top).

Below room temperature, the imino resonances from base pairs (1,10) and (2,9) sharpen and move to lower field, but the terminal base pair imino resonances are still broad at 1 °C due to more rapid exchange with water. Above 24 °C, the A·T imino resonance from base pairs (3,8) begins to broaden and disappear, followed by the resonance from base pairs (4,7). Finally, at 43 °C, both the A·T and G·C imino resonances appear only as broad peaks. A plot of the chemical shift of these resonances as a function of temperature is given in Figure 2. The A·T imino proton resonances shift slowly upfield throughout the temperature range studied. In contrast, the G·C resonances do not shift at all below 30 and 35 °C in the "CG" and the "GC" decamers, respectively, and then shift only slightly.

*Imino Proton Relaxation Measurements.* Spin–lattice relaxation rates were obtained by using the modified time-shared Redfield 214 pulse method (Wright et al., 1981), and these results are summarized in Table I. Relaxation rates are given only for the interior base pair imino protons, since the imino resonances from the terminal and next-to-terminal base pairs have broadened to base line by 20 °C. The spin–lattice relaxation of the internal imino protons is nonexponential at lower temperatures due to spin diffusion (Assa-Munt et al., 1981; Kearns et al., 1981). Therefore, in order to obtain meaningful results, theoretical analysis indicates that initial rates must be measured for the lower temperature experiments (Assa-Munt et al., 1984; Kearns et al., 1981). However, because of fluctuations in the base line at very short $\tau$ values, we did not use data points below ~20 ms, but this should not significantly affect the values obtained since the observed "initial" rates were ~5 $s^{-1}$ (see Table I). We note that the initial rates obtained using the long pulse or time-shared Redfield 214 pulse method may actually be too small (by up to 30%) due to partial polarization of the neighboring amino and AH2 protons during the application of the 180° pulse (R. W. Behling, unpublished results). At low temperatures, the relaxation of imino protons in DNA and tRNA has been shown to be dominated by dipole–dipole interactions (Early et al., 1981a; Johnston & Redfield, 1977), and this is confirmed by relaxation measurements on a sample in 75% $D_2O$. Plots of the 10 and 22 °C relaxation data for the $G{\cdot}C_{(5,6)}$, $A{\cdot}T_{(4,7)}$, and $A{\cdot}T_{(3,8)}$ imino protons of d(ATATCGATAT) in 75% $D_2O$ and 100% $H_2O$ are compared in Figure 3. Large differences in the relaxation times are seen, particularly for the G·C imino protons, when the sample is in 75% $D_2O$ vs. 100% $H_2O$, and these differences become larger at the lower temperature. At high temperatures (above 30 °C for these samples) exchange dominates the relaxation, and the decay is single exponential. If it is assumed that the rate of exchange of the imino protons with water is open limited (i.e., exchange of solvent takes place each time the base pair opens), then these rates are a direct measure of the rate at which base pairs in the helix transiently open (Hilbers, 1979). If this assumption is incorrect (i.e., the base pair opens and closes many times before exchange with solvent), then the rates obtained give only a lower limit for rate of base pair opening in the molecule.

Apparent activation energies for exchange of the imino protons with water can be obtained from the high-temperature limiting slopes of semilog plots of relaxation rates vs. the reciprocal of the absolute temperature (Early et al., 1981a) (Figure 4), and these values for the imino protons of the six

Table I: Spin–Lattice Relaxation Rates[a] ($s^{-1}$) for the Low-Field Resonances of $d(ATATCGATAT)_2$ and $d(ATATGCATAT)_2$

| T (°C) | $d(ATATGCATAT)_2$ | | | $d(ATATCGATAT)_2$ | | |
|---|---|---|---|---|---|---|
| | $A{\cdot}T_{(3,8)}$ | $A{\cdot}T_{(4,7)}$ | $G{\cdot}C_{(5,6)}$ | $A{\cdot}T_{(3,8)}$ | $A{\cdot}T_{(4,7)}$ | $G{\cdot}C_{(5,6)}$ |
| 10 | 5.5 | 5.0 | 5.2 | 4.9 | 5.2 | 5.0 |
| 15 | 6.1 | 4.1 | 4.4 | 6.2 | 4.7 | 3.9 |
| 22 | 13.1 | 5.2 | 3.9 | 12.3 | 7.2 | 4.0 |
| 26 | | | | 18 | 9.5 | 4.5 |
| 28 | 23 | 11 | 5.8 | 22 | 12 | 5.2 |
| 34 | 64 | 35 | 20 | 69 | 34 | 17 |
| 38 | 141 | 98 | 63 | 146 | 84 | 51 |
| 42 | | 218 | 191 | | 230 | 176 |
| | | | 75% $D_2O$[b] | | | |
| 10 | 3.8 | 3.6 | 2.5 | | | |
| 22 | 9.0 | 4.7 | 2.1 | | | |

[a] "Initial value" calculated by using decay data obtained after 20 ms. [b] Relaxation measurements on a sample in 75% $D_2O$.

Table II: Apparent Activation Energies for Exchange (kcal/mol) of Imino Protons in $d(ATATCGATAT)_2$ and $d(ATATGCATAT)_2$

| base pair | $d(ATATCGATAT)_2$ | $d(ATATGCATAT)_2$ |
|---|---|---|
| $A{\cdot}T_{(3,8)}$ | 37 | 36 |
| $A{\cdot}T_{(4,7)}$ | 48 | 46 |
| $G{\cdot}C_{(5,6)}$ | 63 | 64 |

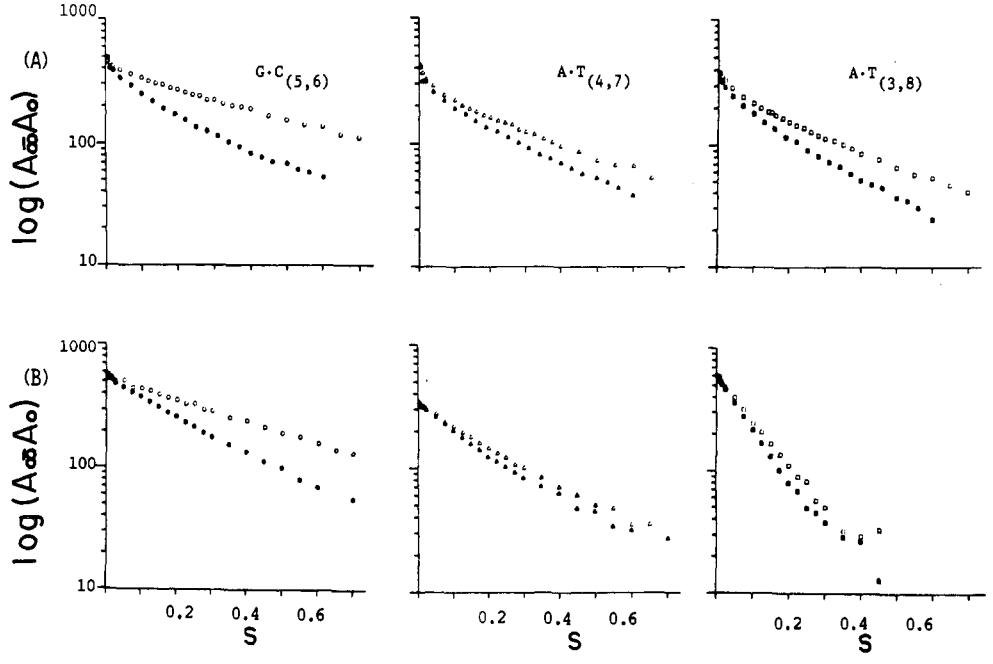


FIGURE 3: Comparison of the imino proton spin–lattice relaxation data obtained for d(ATATGCATAT) in 100% $H_2O$ vs. 75% $D_2O$ at (A) 10 °C and (B) 22 °C. Plots of log $(A_\infty - A_\tau)$ vs. $\tau$ for the imino protons of $G{\cdot}C_{(5,6)}$, $A{\cdot}T_{(4,7)}$, and $A{\cdot}T_{(3,8)}$ are shown. Open symbols, 75% $D_2O$; closed symbols, 100% $H_2O$.

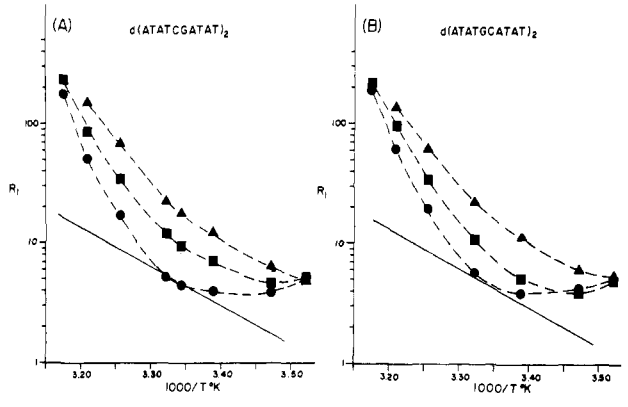


FIGURE 4: Plot of ln $R_1$ vs. $1/T$ (K) for the imino protons of $G{\cdot}C_{(5,6)}$ (●), $A{\cdot}T_{(4,7)}$ (■), and $A{\cdot}T_{(3,8)}$ (▲) in (A) d(ATATCGATAT) and (B) d(ATATGCATAT). Apparent activation energies for exchange of the imino protons with solvent can be obtained from the limiting slope of the high-temperature data. The solid line is a theoretical curve for the A·T exchange rate $k_{ex} = (2 \times 10^{12})e^{-\Delta H/(RT)}$, where $\Delta H$ = 16 kcal, derived from other studies (Kearns et al., 1981).

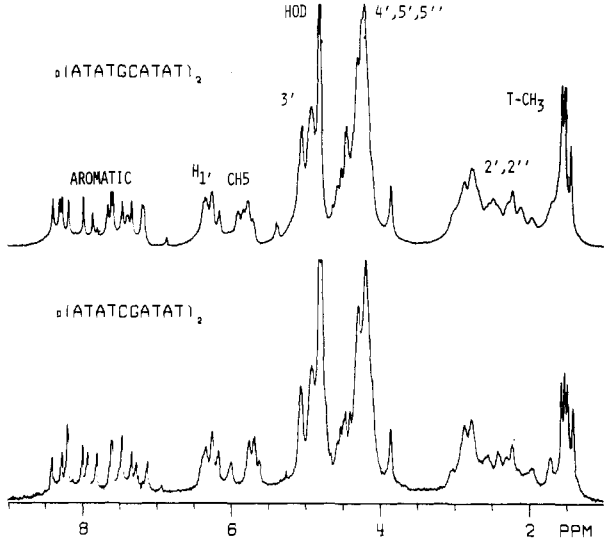


FIGURE 5: 360-MHz spectra of d(ATATGCATAT) and d(ATATCGATAT) in $D_2O$ at 29 °C. Assignments to general proton type are given above the spectra. Spectra are line broadened (exponential multiplication) by 2 Hz.

interior base pairs in the two molecules are summarized in Table II.

*(B) Spectra of the Nonexchangeable Protons. General Assignments.* NMR spectra of the nonexchangeable protons in the two decamers d(ATATCGATAT) and d(ATATGCATAT) at 29 °C are presented in Figure 5, along with assignments to proton type(s). The decamers are still fully double stranded at this temperature, as evidenced by a temperature study of the chemical shifts and line widths of the resonances (see below).

*Assignment of Aromatic Resonances to Proton Type.* Figure 6 shows the aromatic spectra of d(ATATCGATAT) at 20 °C. Assignment of aromatic resonances to type of protons is relatively straightforward. The AH8 protons have the lowest field intrinsic positions and receive only small ring current shifts from neighboring base pairs (Patel & Tonelli, 1974; Arter & Schmidt, 1976; Patel & Canuel, 1976a,b; Early et al., 1977). The GH8's are expected to resonate further upfield between 8.0 and 7.8 ppm. The GH8 and AH8 protons can readily be distinguished from all other aromatic protons, since they exchange with $D_2O$ on heating (Schweizer et al., 1964), as illustrated in the inset to Figure 6. By following the disappearance of the peaks with time, the more rapidly exchanging GH8 protons can be distinguished from the AH8 protons. The AH2 protons have the longest $T_2$'s (see below) and can easily be identified in a partially relaxed $T_2$ spectrum (Early et al., 1980) (see inset B to Figure 6). The CH6 and TH6 resonances between 7.5 and 7.0 ppm are easily distinguished from each other since the CH6 protons are split by ~7.5 Hz by their neighboring CH5's and appear as doublets. In the "GC" decamer the CH6 resonance is obscured by a TH6 resonance at 20 °C but is resolved at higher temperature. It can also be seen as an inverted peak in the spin-echo experiments described below.

*Assignments of Aromatic Resonances to Specific Base Pairs.* The similarities and differences between the two de-

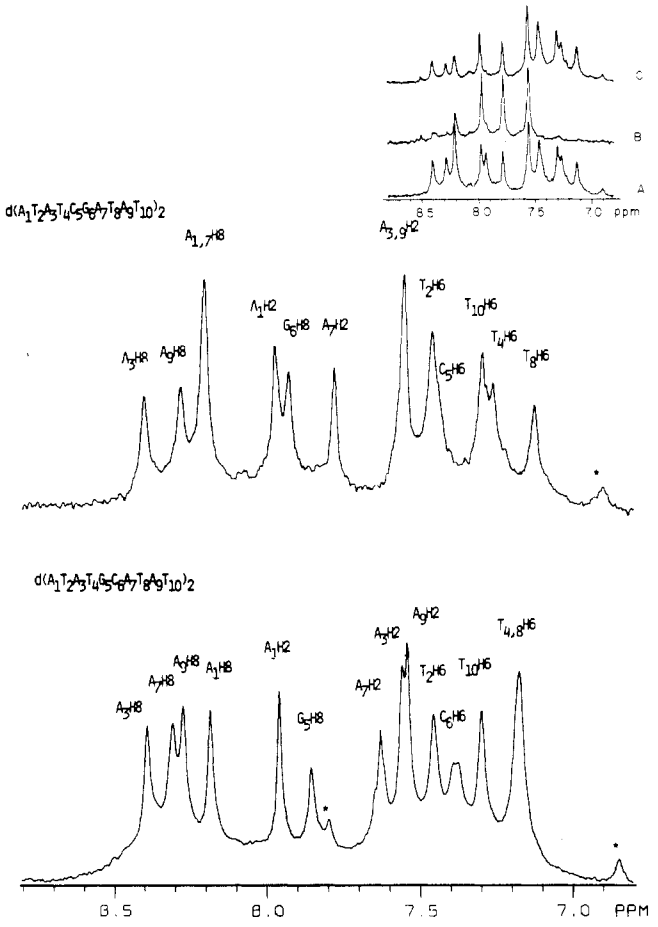


FIGURE 6: 360-MHz aromatic spectra of d(ATATCGATAT) and d(ATATGCATAT) in $D_2O$ at 20 °C. Specific proton assignments, as well as chemical shifts, are given over each peak; for discussion of these assignments, see text and Feigon et al. (1983). Starred peaks are impurities which probably arise from incomplete cleavage of blocking groups. The inset to the figure illustrates some of the methods used to assign protons to type, i.e., AH8, GH8, TH6, CH6, or AH2: (A) Normal spectrum of d(ATATCGATAT) and (B) partially relaxed $T_2$ Hahn spin-echo spectrum ($\tau$ = 130 ms). Most of the resonances have decayed to base line, while resonance intensity from the four AH2 resonances (the resonance at 7.55 ppm corresponds to two protons) remains, along with some intensity from the terminal AH8. (C) Aromatic spectrum obtained after heating the sample in $D_2O$ for 1.5 h at 100 °C. The GH8 resonance at 7.92 has completely disappeared, and intensity of the AH8 resonances is greatly reduced due to chemical exchange with deuterium. The terminal AH8 exchanges faster than the interior AH8's.

camers were exploited to assign the AH8, AH2, and TH6 resonances to specific bases. [Since the two G·C base pairs in each molecule are equivalent, the GH8 and CH6 resonances were automatically assigned to base pairs (5,6).] In making assignments, it was assumed that resonances from the terminal and next-to-terminal base pairs [(1,10) and (2,9), respectively] have the same chemical shifts for both molecules, resonances from base pairs (3,8) might have somewhat different chemical shifts in the two molecules, and the resonances from base pairs (4,7) next to the G·C base pairs could have quite different chemical shifts in the two decamers. Comparison of the spectra of the two decamers, combined with the $T_2$ data, rates of chemical exchange with deuterium, qualitative ring current considerations, and nuclear Overhauser effects (NOEs) (see below) permitted the assignment of most of the aromatic protons at 20 °C.

Those aromatic resonances that can be assigned for both decamers by using just the data presented in this paper are summarized in Table III. Referring to Figure 6, it can be

Table III: Aromatic Proton Resonance Assignments in $d(ATATCGATAT)_2$ and $d(ATATGCATAT)_2$ Based on One-Dimensional Data Only[a]

| | $d(ATATCGATAT)_2$ | | $d(ATATGCATAT)_2$ | |
|---|---|---|---|---|
| type | ppm[b] | base | ppm[b] | base |
| AH8 | 8.39 | 3 or 9 | 8.39 | 3 or 9 |
| | 8.26 | 3 or 9 | 8.30 | 7 |
| | 8.19 | 7 | 8.27 | 3 or 9 |
| | 8.19 | 1 | 8.18 | 1 |
| AH2 | 7.97 | 1 | 7.95 | 1 |
| | 7.77 | 7 | 7.62 | 7 |
| | 7.55 | 3, 9 | 7.55 | 3 |
| | 7.55 | 3, 9 | 7.54 | 9 |
| TH6 | 7.46 | 2 or 10 | 7.45 | 2 or 10 |
| | 7.30 | 2 or 10 | 7.29 | 2 or 10 |
| | 7.26 | 4 or 8 | 7.17 | 4 or 8 |
| | 7.12 | 4 or 8 | 7.17 | 4 or 8 |
| GH8 | 7.92 | 6 | 7.85 | 5 |
| CH6 | 7.4 | 5 | 7.3 | 6 |

[a] Complete assignments of the AH8 and TH6 resonances were made by using the results of the 2D NOE experiments described in the following paper (Feigon et al., 1983) and are given in Figure 6. [b] $T$ = 20 °C.

seen that the major difference between the AH8 spectral region in the two decamers is that the "CG" decamer has intensity corresponding to two resonances (four protons) at 8.19 ppm while the "GC" decamer has one resonance at 8.19 ppm and another at 8.30 ppm. This indicates that the AH8 resonance from base 7 is at 8.30 ppm in the "GC" decamer and is one of the two resonances at 8.19 ppm in the "CG" decamer. The terminal AH8 in both decamers resonates at ~8.18 ppm; this assignment is substantiated by their long $T_2$'s and their faster exchange with $D_2O$ on heating, as compared with interior AH8's. The other two AH8 resonances in each molecule are from bases 9 and 3 and cannot be definitively assigned by this method alone.

The terminal and next-to-terminal TH6 resonances can be assigned in both decamers on the basis of their identical chemical shifts in both molecules, but they are only tentatively distinguished from each other on the basis of the slightly longer $T_2$ for the terminal base pair resonance. The chemical shifts for the two more interior base pairs are significantly different in the two decamers, so they cannot be specifically assigned. Confirmation of and completion of the assignments for the AH8 and TH6, as well as the thymine methyl, resonances were made by using the results of two-dimensional NOE experiments (Feigon et al., 1982, 1983).

Considerations similar to those above, as well as NOE experiments, were used to assign the AH2 resonances Since the AH2's receive large ring current shifts, it is expected that the AH2 at lowest field would be from the terminal base pair. The peak at 7.77 ppm in the "CG" decamer is assigned to base 7, because it has the largest chemical shift difference from the other AH2's in the "GC" decamer. The peak at 7.55 ppm is assigned to bases 9 and 3. For the "GC" decamer, the peak at 7.62 ppm can be tentatively assigned to base 7, and this assignment is confirmed by the NOE experiments described below.

*Nuclear Overhauser Effect Measurements.* The AH2 protons can be independently assigned by using saturation-transfer experiments to observe nuclear Overhauser effects in water (Sanchez et al., 1980; Redfield et al., 1981). In $H_2O$, the closet proton to an AH2 proton is the T imino proton located at a distance of ~2.85 Å (Taylor & Kennard, 1982; R. W. Behling, unpublished results). Since the imino protons are unambiguously assigned, saturation transfer to the AH2's

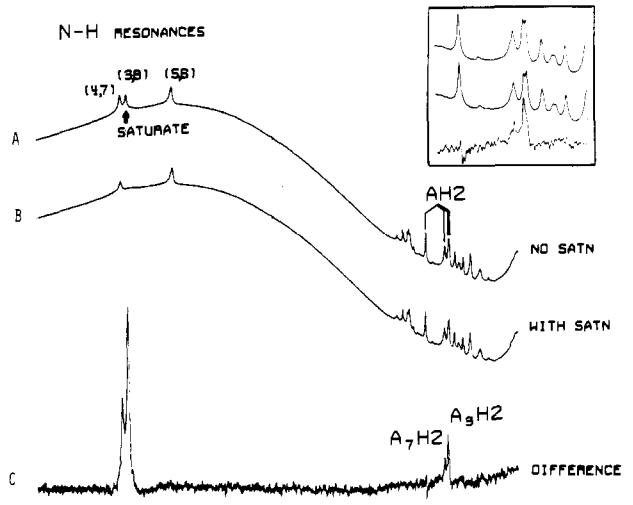


FIGURE 7: Nuclear Overhauser effect between the thymine imino proton resonance from base pairs (3,8) and the $A_3H2$ resonance in d(ATATGCATAT) in $H_2O$ at 20 °C. A saturating pulse of 300 ms was applied through the decoupler, followed by a time-shared Redfield 214 observe pulse (Wright et al., 1981). (A) The saturating pulse is applied to a resonance-free region (downfield of the imino protons). (B) The saturating pulse is applied at the resonance position of the imino proton of base pairs (3,8) (shown with arrow). The neighboring imino proton resonance from base pairs (4,7) is also partially saturated by this pulse, so its intensity is reduced. (C) The difference spectrum of (A) and (B) shows a large negative NOE at one AH2 resonance, which can therefore be assigned to $A_3H2$. The smaller NOE is due to partial saturation of the imino resonance from base pairs (4,7) and is assigned to $A_7H2$. Another experiment involving full saturation of the imino resonance from base pairs (4,7) confirmed these assignments (not shown). In the inset to the figure, the region of the spectrum containing the AH2 resonances is expanded to show that the larger NOE occurs at the lower field resonance of the two partially overlapping AH2 resonances. The GH8 and, to a larger extent, the AH8 protons in this sample had been chemically exchanged with deuterium prior to this experiment and are therefore missing from the spectrum. New resonances which are absent in the aromatic spectrum in $D_2O$ are due to protons on the amino groups.

allows the latter to be assigned also (Sanchez et al., 1980). This method was used to assign the AH2 resonances of interior A·T base pairs in both decamers.

An example of a saturation transfer experiment on the GC decamer is given in Figure 7, where the imino proton resonance from base pairs (3,8) is selectively saturated. Because of overlap of the imino proton resonances it was not possible to saturate the resonance from base pairs (3,8) without slightly affecting the neighboring resonance, and consequently negative NOEs for two AH2 resonances are observed in the difference spectrum. The largest absolute intensity is observed for the AH2 at 7.55 ppm and is assigned to $A_3H2$, while the downfield peak at 7.62 ppm is assigned to $A_7H2$.

*Temperature Dependence of the Aromatic Spectra.* Plots of the chemical shifts vs. temperature are given in Figure 8 for the aromatic protons of d(ATATCGATAT) and d(ATATGCATAT), respectively. The GH8 as well as the terminal AH8 resonances could be followed unambiguously through the crossovers that occurred during the duplex-to-strand transition by their absence after exchange with $D_2O$. Some AH2 resonances could not be followed unambiguously since the NOE experiments cannot be done at high temperature due to exchange of the imino protons with $H_2O$; therefore, those specific assignments at high temperature are tentative.

The chemical shifts for most of the protons remain fairly constant until ~40 °C, when the resonances begin to shift, generally to lower field. The AH2 resonances shift most dramatically with temperature, since they are the most ring

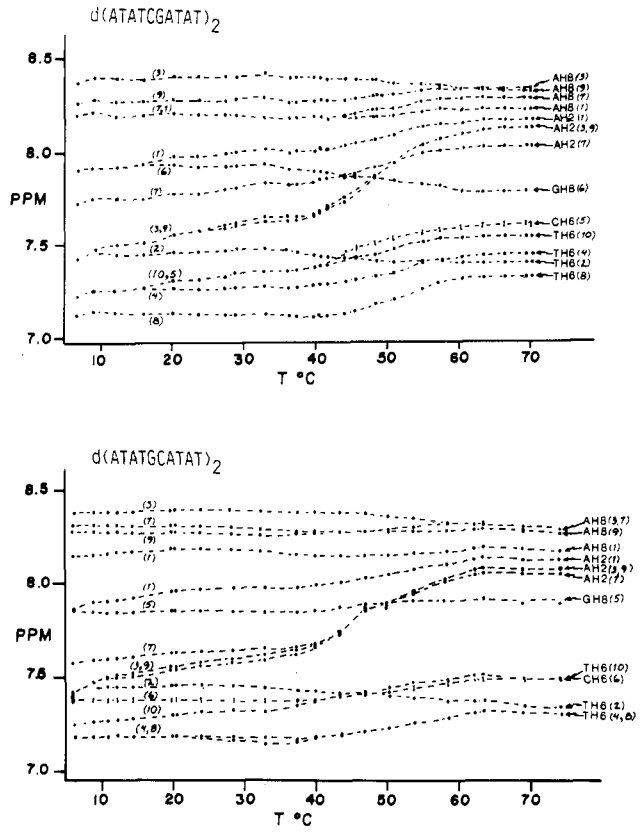


FIGURE 8: Plot of the chemical shifts of the aromatic proton resonances of d(ATATCGATAT) (top) and d(ATATGCATAT) (bottom) in $D_2O$ at 360 MHz as a function of temperature. The assignments given are discussed in the text. The high-temperature assignments of the $A_{3,9}H8$ resonances in d(ATATCGATAT) and in d(ATATGCATAT) are tentative (with respect to base, but not with respect to proton type).

current shifted in the double-stranded state. Above ~60 °C, the chemical shifts of the resonances again become fairly constant. The plots of the chemical shifts of the aromatic proton resonances as a function of temperature can be used to estimate the midpoint of the helix-to-coil transition ($T_m$) (Borer et al., 1975; Patel, 1975; Kan et al., 1975). With the possible exception of the terminal base pairs, no differential melting was observed in either of the two molecules. Transition midpoints of 50 ± 2 and 52 ± 2 °C were obtained for d(ATATCGATAT) and d(ATATGCATAT), respectively.

Although most of the base proton resonances shift downfield during the helix-to-coil transition, upfield shifts are observed for some of the base proton resonances; in particular, the $G_6H8$, $T_2H6$, and $A_3H8$ resonances of the "CG" decamer and the $T_2H6$ and $A_3H8$ resonances of the "GC" decamer.

Some aspects of the spectral changes that occur with changes in temperature which are not evident in the chemical shift plots can be observed in Figure 9, which shows the aromatic spectra of d(ATATGCATAT) at several different temperatures. At low temperatures, the line widths of the aromatic and methyl resonances (not shown) are fairly broad, but they sharpen up as the temperature is raised above 10 °C; this broadening at low temperatures is attributed to a reduction in molecular tumbling rates due to increased solution viscosity and/or aggregation of the DNA decamers. Between 10 and 37 °C the line widths remain sharp, but above 37 °C several resonances broaden again. Those resonances which shift the most are also the most broadened, and this makes it difficult to follow some of the resonances through the melting transition. For instance, at 43 °C, three of the AH2 resonances in the "CG" decamer appear as one very broad resonance centered at 7.73 ppm (Figure 9). The amount of broadening of each

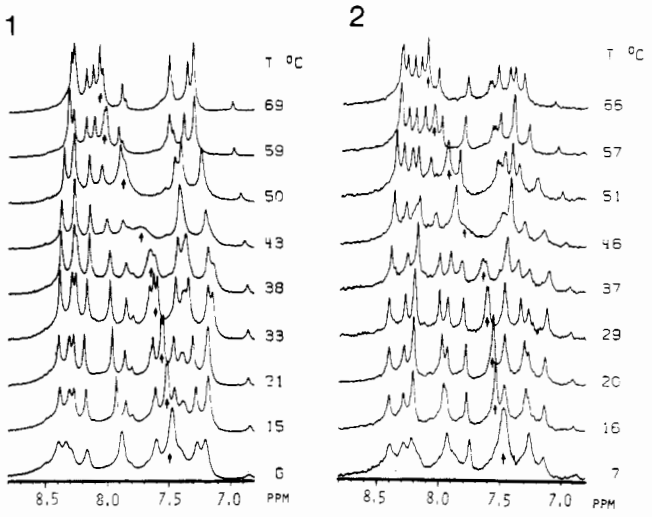


FIGURE 9: 360-MHz spectra of the aromatic region of (1) d(ATATGCATAT) and (2) d(ATATCGATAT) as a function of temperature. The arrows follow the movement of the $A_{3,9}H2$ proton resonances. All spectra are plotted with the same maximum peak height.

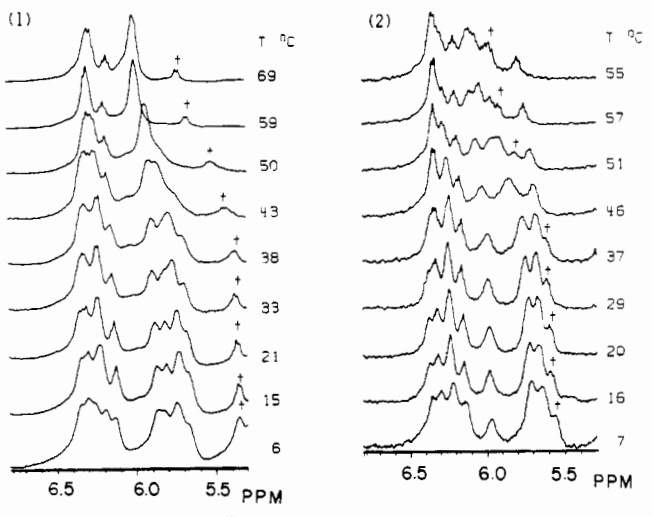


FIGURE 10: 360-MHz spectra of the deoxyribose H1′, CH5 region of (1) d(ATATGCATAT) and (2) d(ATATCGATAT) as a function of temperature. Daggers (†) indicate the position of the CH5 resonance.

resonance during the melting transition depends on the magnitude of the chemical shift difference between the double-stranded and single-stranded states, the rate of exchange, and the population difference between the helix and coil at any given temperature (Gutowsky & Holm, 1956). If the exchange rate between helix and coil is in the fast-exchange limit on the NMR time scale, then the resonance will remain sharp, and the resonance position will be the population weighted average of the resonance positions in helix and coil. However, if the exchange rate is intermediate, then uncertainty broadening of the resonances will occur, and resonances with the largest chemical shift difference between helix and coil will be the most broadened. In and near the slow-exchange limit, two separate resonances will appear for each proton with intensities proportional to the population difference between helix and coil. The extensive broadening which is observed for many of the aromatic resonances in the DNA decamers at around 43 °C indicates that the exchange between helix and coil is not in the fast-exchange limit below the $T_m$.

*The Deoxyribose H1′ and CH5 Region.* The deoxyribose H1′ and CH5 region is shown at several temperatures for the two decamers in Figure 10. At ~30 °C the doublet from the CH5 is clearly visible at 5.37 ppm in the "GC" decamer and is less clearly distinguished at 5.61 ppm from the H1′ resonances in the "CG" decamer. At higher temperatures the CH5 resonances shift downfield and are difficult to resolve from the H1′ resonances. The H1′ protons are coupled to H2′ and H2″ and appear as a collection of partially resolved pseudotriplets. Resolution-enhanced spectra at three temperatures are presented in Figure 11, and coupling constants deduced from these spectra are summarized in Table IV.

Although the H1′ regions of the two decamers can be compared for similarities and differences, the methods outlined in the preceding sections cannot be used to make assignments, since assignments to base type (A, T, C, or G) are not known. Assignments of the H1′ sugar resonances, discussed in the following paper (Feigon et al., 1983), rely on the results of 2D-NOE experiments.

*Spin-Echo Experiments: Determination of Coupling Constants.* The results of a Hahn spin-echo ($T_2$) experiment on d(ATATCGATAT) are shown in Figure 12 for the spectral region from ~5 to 9 ppm. For most of the aromatic region, the intensities of the peaks decrease exponentially with time,

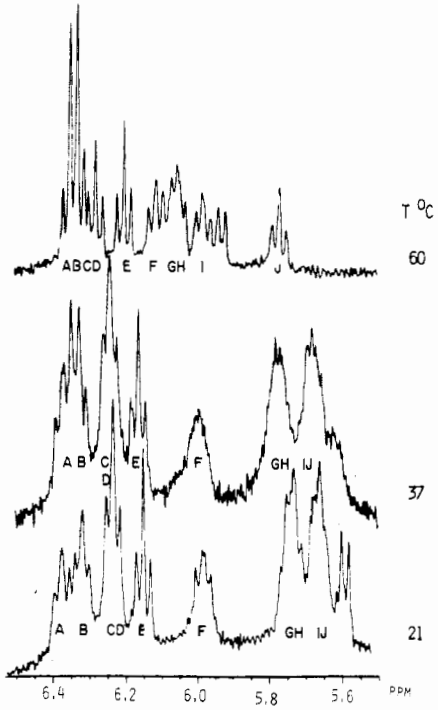


FIGURE 11: Resolution-enhanced 360-MHz spectra of the deoxyribose H1′, CH5 region of d(ATATCGATAT) at 21, 37, and 60 °C. A total of 128 transients was collected with a 9-μs pulse and a 4-s acquisition time. Spectra were resolution enhanced by double-exponential multiplication of the FID. H1′ resonances are identified by letters A–J, although the letters assigned to a particular peak may not be the same at high and low temperature. The measured coupling constants are given in Table IV. All spectra are shown plotted with the same maximum peak height.

and spin–spin relaxation times can be directly calculated by appropriate analysis of the decay curves (see Table V). A much different behavior is observed for the homonuclear coupled deoxyribose H1′, CH5, and CH6 protons. The H1′ resonances in the 10-, 20-, and 30-ms spectra look resolved due to an "apparent" decoupling from the H2′,H2″ protons, while the CH5 resonance, along with the CH6 resonance which is partially buried beneath a TH6 resonance, inverts at 60 ms. As shown by Hahn & Maxwell (1952), homonuclear, scalar coupling of spins leads to a modulation of the decay, and this can be exploited to obtain coupling constants. Theory predicts that for two coupled protons, the doublets will invert at $t_1$ =

Table IV: Summary of the H1′ Proton Chemical Shifts and Coupling Constants for Spectra Shown in Figure 11

| $T$ (°C) | sugar[a] | chemical shift | measured splittings (Hz) | $J_{1'2'} + J_{1'2''}$ |
|---|---|---|---|---|
| 21 | A | 6.37 | 7.3, 7.1 | 14.4 |
| | B | 6.31 | 7.3, 6.3 | 13.6 |
| | C, D | (6.23) | (6.5, 6.7) | (13.2) |
| | E | 6.14 | 7.1, 6.9 | 14.0 |
| | F | 5.98 | 6.7, 6.0, 2.1 | 14.8 |
| | G, H | 5.72 | | |
| | I, J | 5.65 | | |
| 37 | A | 6.34 | 8.4, 7.1 | 15.5 |
| | B | 6.32 | 7.9, 6.4 | 14.3 |
| | C, D | (6.23) | (5.9, 6.5) | (12.4) |
| | E | 6.16 | 7.9, 6.7 | 14.6 |
| | F | 5.99 | | |
| | G, H | 5.76 | | |
| | I, J | 5.67 | | |
| 60 | A | 6.34 | 6.6, 6.9 | 13.5 |
| | B, C | (6.33) | (6.9, 6.9) | (13.8) |
| | D | 6.27 | 7.1, 7.3 | 14.4 |
| | (E) | 6.20 | 6.9, 6.8 | 13.7 |
| | (F) | 6.11 | 7.4, 6.8 | 14.2 |
| | (G, H) | (6.05) | (5.8, 8.3) | (14.1) |
| | (I) | 5.98 | 5.8, 8.6 | 14.4 |
| | J | 5.76 | 7.1, 6.5 | 13.6 |

[a] Sugars have been assigned to bases [see Feigon et al. (1983)] at 27 °C as follows: A ($A_3$), B ($A_9$), C, D ($A_1$ and $A_7$), E ($T_{10}$), F ($T_4$), G, H ($T_8$ and $T_2$), and I, J ($G_6$ and $C_5$). (Where two peaks overlap, the coupling constants are approximate, and $J_{1'2'} + J_{1'2''}$ is the maximum possible.)

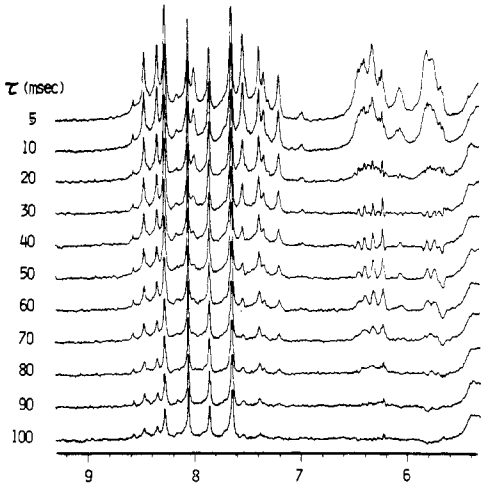


FIGURE 12: Results of a Hahn spin-echo ($T_2$) experiment on d-(ATATCGATAT) at 23 °C are shown for the aromatic and H1′, CH5 regions. The pulse sequence for the experiment was (90–$\tau$–180–$\tau$–acquisition–$D_5$)$_n$ and the delay times ($\tau$) are listed to the left of the spectra. Note that phase modulation is observed for the resonances of the homonuclear-coupled H1′, CH5, and CH6 protons in the 5.5–6.5 ppm region. A 10-s recovery time ($D_5$) was used, and 64 FIDs were accumulated for each $\tau$ value. The spectra are line broadened (exponential multiplication) by 2 Hz.

$^1/_2J$, where $t_1$ is the delay time between the 90° and 180° pulses and $J$ is the coupling constant [see Freeman & Hill (1975)]. At twice this time the resonances should be right side up again, and so on. For a triplet, only the outer two lines will be modulated, and this gives rise to the apparent resolution and "nulling" of the H1′ resonances at $t_1$ values near $^1/_2J$. In both the "CG" and "GC" decamers, the lower field cluster of H1′ resonances have $t_1 \simeq$ 30–35 ms, while for the higher field collection of resonances $t_1 \simeq$ 35–40 ms. This corresponds to coupling constants of 14–17 and 12–14 Hz, respectively. These values are consistent with an S sugar conformation as expected for B-family DNA (see Discussion). Analysis of the coupling constants for the sugar H1′ resonances is complicated by the fact that the center peak of these pseudotriplets is actually split by 0.5–4 Hz (Cheng et al., 1982), leading to further modulations of the spin echoes. It can be seen that the peak height of the single resonance at 6.15 ppm in both the "CG" and "GC" decamers is greater than that for the next most downfield peak which corresponds to *two* H1′ protons, and in fact this higher field resonance is still visible at $t_1$ = 120 ms when the other resonances have decayed to base line. This slower decay is consistent with the (apparently) narrower line width of this resonance, and it is, therefore, tentatively assigned to the terminal T nucleosides. This assignment is confirmed in the 2D-NOE experiments [see Feigon et al. (1983)]. The 6.15 ppm sugar resonance is attributed to the terminal T nucleoside, rather than the terminal A nucleoside, since the stacking energy of A is greater than that for U or T (Romaniuk et al., 1977); therefore, the sugar attached to the T base is more likely to be averaging rapidly enough to give rise to the sharper line.

Table V: Spin-Spin Relaxation Times for d(ATATGCATAT)$_2$ and d(ATATCGATAT)$_2$ at 21 °C

| base | proton | ATATGCATAT[a] $T_2$ (ms) | ATATCGATAT[a] $T_2$ (ms) |
|---|---|---|---|
| 1 | AH8 | 162, 170 | (138), (131), (130) |
| 9 | AH8 | 102, 101 | 108, 106, 109 |
| 3 | AH8 | 98, 106 | 103, 105, 92 |
| 7 | AH8 | 92, 96 | (138), (131), (130) |
| | GH8 | 124, 134 | 130, 153, 151 |
| 1 | AH2 | 322, 335 | 288, 292, 313 |
| 9 | AH2 | (245), (232) | (219), (236), (227) |
| 3 | AH2 | (245), (232) | (219), (236), (227) |
| 7 | AH2 | 311, 316 | 248, 405, 203, 399 |
| 10 | TH6 | 78, 73 | 79, 82, 73 |
| 2 | TH6 | 73, 82 | 47, 64, 73[b] |
| 8 | TH6 | (69), (53) | 65, 67, 59 |
| 4 | TH6 | (69), (53) | 61, 71, 70 |

[a] Values in parentheses indicate the single relaxation time determined for two overlapping resonances. [b] Value inaccurate due to overlap with CH6 resonances.

*Spin–Lattice Relaxation Experiments in $D_2O$.* Nonselective spin–lattice relaxation experiments at 360 MHz on the two decamers gave rates which vary only slightly from ~0.9 $s^{-1}$ for most of the sugar protons to 0.7 $s^{-1}$ for the base and deoxyribose H1′ protons. Only the AH2 protons have a significantly different rate of 0.36 $s^{-1}$ (data not shown). It has previously been shown that nonselective $T_1$'s do not provide meaningful structural information for DNA polymers due to complications from spin diffusion (Early et al., 1980; Kearns et al., 1981; Assa-Munt et al., 1981). Some selective spin–lattice relaxation rate measurements were carried out on the AH2 resonances in the "CG" decamers, and these results are summarized in Table VI.

## Discussion

*Imino Proton Assignments.* A total of five imino proton resonances are expected and observed for each DNA decamer, d(ATATCGATAT) and d(ATATGCATAT), at low temperatures (see Figure 2). The resonances due to the imino protons of the G·C base pair were unambiguously assigned on the basis of their chemical shifts, relaxation rates, and $D_2O$ effect on relaxation; resonances from A·T base pairs were assigned primarily on the basis of their sequential broadening with increasing temperature and also by comparison of the

Table VI: Comparison of Observed and Calculated Relaxation Rates for Selected Protons of d(ATATCGATAT)$_2$[a]

| proton | neighbor proton type | distance (Å) | relaxation rates ($s^{-1}$) calculated | observed[b] |
|---|---|---|---|---|
| TNH | A-$NH_2$ | 2.46 | $R_1 = 2.1$[c] | $R_1 = 2.6$-4.0[d,e] |
| | AH2 | 2.85 | $R_2 = 10.5$ | $R_2 = 17 \pm 2$[d] |
| | distant protons | | | |
| GNH | C-$NH_2$ | 2.2 | $R_1 = 3.6$[c] | $R_1 = 5.0$[e] |
| | G-$NH_2$ | 2.45 | $R_2 = 18$ | $R_2 = 20$ |
| | distant protons | | | |
| GH8 | H2′ | 2.2 | $R_1 = 3.8$[g] | $R_1 = f$ |
| | H2″ | 2.2 or 2.0 and 2.8 | $R_2 = 7.6$[g] | $R_2 \simeq 7$ |
| AH8 | H2′ | 2.2 | $R_1 = 4.6$[h] | $R_1 = 2.6 \pm 0.5$ |
| | H2″ | 2.2 | $R_2 = 9.1$[h] | $R_2 = 9$-10 |
| | T-$CH_3$ | 3.1 | $R_2 = 1.5$-2[j] | $R_2 = 2$-3[i] |
| TH6 | T-$CH_3$ | 2.8 | $R_1 = 1.6$[l]$R$ | $R_1 = f$ |
| | | | $R_2 = 3.2$[l] | $R_2 = 7$[k] |
| AH2 | AH2 | 2.7 | $R_1 = 0.0$ | $R_1 = 0$[n] |
| | | | $R_2 = 1.0$ | $R_2 = 1.2$[n] |

[a] Calculated by using $\tau_c = 6$ ns, $f_1 = 0.65$, and $f_2 = 0.50$ (see text). [b] 22 °C data. [c] $R_1^{calcd}$ values increased by 0.9 $s^{-1}$ and $R_2^{calcd}$ values increased by 1.8 $s^{-1}$ to account for interactions with more distant nonneighbor protons. Nitrogen contribution to $R_2$ relaxation rates also included. [d] Observed values corrected for an exchange contribution of ~3 $s^{-1}$. [e] True $R_1$ rates may be faster due to nonselective character of excitation (180°) pulse. [f] Not measured. [g] Relaxation rates due entirely to two closest sugar protons. [h] Includes contributions from closest sugar proton and T-$CH_3$. [i] Contribution to $R_2$ from T-$CH_3$; taken as difference between $R_2$ (total) for AH8 and GH8. [j] The T-$CH_3$ contributions to $R_2$. [k] Contributions to $R_2$ from T-$CH_3$; taken as difference between $R_2$ (total) for TH6 and GH8. [l] T-$CH_3$ contribution to $R_{1,2}$. [m] AH2-AH2 contribution; obtained as the difference between $R_{1,2}$ measured for $A_3$, $A_9$ and for $A_7$.

spectra of the two molecules. The former method of assignment assumes that breathing rates (exchange rate with water) of the base pairs in the molecule decrease inwardly from the ends of the duplex and increase sequentially with temperature (Kan et al., 1975; Patel, 1975). While this is no doubt a valid assumption for these molecules, it is not necessarily expected to be true for longer and/or more G·C-rich molecules.

*Temperature Dependence of the Imino Spectra.* The broadening and disappearance of the imino proton resonances from terminal base pairs prior to those from the rest of the molecule has been observed in several molecules (Patel & Hilbers, 1975; Kan et al., 1975; Kallenbach et al., 1976; Early et al., 1981a; Pardi et al., 1981; Pardi & Tinoco, 1982). This is generally attributed to fraying which is characterized as a rapid equilibrium between base-paired and opened states, with base-catalyzed exchange with the solvent occurring from the open state (Patel & Hilbers, 1975).

The chemical shifts of A·T resonances are very temperature sensitive. Resonances from the A·T base pairs (3,8) and (4,7) shift upfield almost linearly with temperature until about 40 °C where they are broadened almost to base line. Resonances from base pairs (1,10) and (2,9) also shift upfield, but they disappear at lower temperatures. In contrast, the G·C imino proton resonances do not shift at all, until at least 30 °C, and then only slightly. NMR studies on a G·C-rich 12 base pair restriction fragment (Early et al., 1981a) and the self-complementary decamer d(CGCGAATTCGCG) (Patel et al., 1982a–d) reveal similarly large temperature-dependent chemical shifts for the interior A·T imino protons in those molecules and only small temperature-dependent chemical shifts of the G·C imino protons. The shift of the A·T imino proton resonance with temperature has been tentatively attributed to "cracking" of the A·T base pairs (transient disruption of the imino H bond without exchange or formation of a new H bond with water) by Early et al. (1981a) and to a sequence-dependent conformational change such as base pair propeller twisting and/or duplex unwinding in the AATT center of the duplex studied by Patel et al. (1982a–d). The similar chemical shift patterns observed in these different molecules, including a 12 base pair restriction fragment where two of the A·Ts have G·C neighbors in both sides, argue against attributing the temperature effect to a sequence-dependent conformational change. Rather, it suggests that the different behavior of the A·T and G·C imino protons with temperature may reflect differences in the hydrogen bond strengths of G·C and A·T base pairs.

*Imino Proton Spin–Lattice Relaxation Data.* The spin–lattice relaxation data for the G·C and A·T imino protons of DNA show a strong temperature dependence, as illustrated in Figure 4. At low temperatures, spin–lattice relaxation rates for the imino protons in DNA are dominated by magnetic dipole–dipole interactions, while exchange of imino protons with water molecules dominates the high-temperature relaxation rates (Early et al., 1981a; Johnston & Redfield, 1977).

(*1*) *Low-Temperature Behavior.* Both the A·T and G·C resonances exhibit nonexponential recovery of their longitudinal magnetization up to temperatures (22 °C) where exchange begins to contribute significantly to the relaxation. This nonexponential decay at lower temperatures is to be expected as a result of spin diffusion (Kearns, 1983). The very significant effect of 75% $D_2O$ on the relaxation behavior of the imino protons, illustrated in Figure 3, confirms that dipole–dipole interactions with neighboring protons are a major factor in the relaxation of the imino protons at low temperatures. As expected, the effect is larger for the G·C imino protons than the A·T imino protons. While quantitative evaluation of the relaxation data in 75% $D_2O$ is difficult, because there will be several rates depending on the number of protons replaced by deuterons for a given base pair, a qualitative comparison can be made by measuring the relaxation between $\tau = \sim 50$ and 150 ms, and the results for the "GC" decamer are given in Table I. The rates for the G·C imino protons decrease by a factor of 2 on going from $H_2O$ to 75% $D_2O$ at 10 °C, while those of the A·T imino protons only decrease by about 30%. At 22 °C the relative difference in the rates in $H_2O$ and 75% $D_2O$ decreases, especially for the A·T imino protons, since exchange is beginning to contribute to the relaxation at this temperature. A theoretical analysis of the imino proton spin–lattice and spin–spin relaxation rates will be given below when we consider the magnetic dipole induced relaxation behavior of the *non*exchangeable protons.

(*2*) *High-Temperature Relaxation Behavior.* At high temperatures, exchange of the imino protons with solvent protons dominates their relaxation, and under these conditions the A·T and G·C resonances exhibit exponential decay. The rates obtained for the imino protons of base pairs (3,8), (4,7), and (5,6) in d(ATATGCATAT) and d(ATATCGATAT) are the same within experimental error for the respective base pairs of each molecule (Table I). Activation energies of 36 ± 2, 47 ± 2, and 64 ± 2 kcal/mol were obtained for the imino protons of the A·$T_{(3,8)}$, A·$T_{(4,7)}$, and G·$C_{(5,6)}$ base pairs, respectively, in both decamers. Thus, the apparent activation energies increase toward the center of the duplex, and they are higher than those obtained in the other molecules. For example, the activation energy for exchange of T imino protons is 16 ± 2 kcal/mol in three short (12, 43, and 69 base pair) restriction fragments (Early et al., 1981b) and in poly(dA-dT) (Kearns et al., 1981; Assa-Munt et al., 1981). The activation

energy for exchange of G imino protons in poly(dG-dC) is only ~20 kcal/mol (Mirau & Kearns, 1983). These results indicate that in the longer polymers, exchange of the imino protons with solvent takes place primarily as a single base pair phenomenon. However, if the rate for partial, or complete, opening of the helix is faster than the rate for opening a single base pair within the helix, then the activation energy would be larger and possibly temperature dependent. Therefore, the activation energy of 64 kcal/mol obtained for exchange of the $G{\cdot}C_{(5,6)}$ imino protons in the decamers studied here probably represents the activation energy for disruption of the entire helix. Similarly high activation energies for exchange were observed for the interior imino protons in $d(CA_5G){\cdot}d(CT_5G)$, and the authors concluded that the activation energy represented the activation energy for the opening of the entire helix (Pardi et al., 1982). Values of 36 and 47 kcal which we observe for the apparent activation energies for exchange of the $A{\cdot}T_{(3,8)}$ and $A{\cdot}T_{(4,7)}$ imino protons, respectively, may be due to contributions from single base pair opening, partial helix opening, and complete helix opening and cannot be more thoroughly evaluated from the data presented here.

*Aromatic Resonance Assignments.* By use of chemical shifts, relative relaxation rates, deuterium exchange, and coupling constants, all of the base protons of the two decamers can be unambiguously assigned as to proton type, and these are summarized in Figure 6. The basic approach in making the assignments to specific base pairs was to assume that the chemical shifts of the resonances from the terminal and next-to-terminal A·T base pairs would be the same for both molecules, while the chemical shifts for the resonances from the more interior base pairs might be different for the two decamers, with the largest differences expected for the A·T base pair next to the G·C base pair. The implicit assumption is that structural differences between the two molecules, if any, would not propagate past base pairs (4,7) and (5,6). Since the terminal AH8 and all of the AH2 resonances can be unambiguously assigned by other criteria, it seems very unlikely that this assumption is in error. Moreover, the spectra of the imino proton resonances are also consistent with the assumption of similar conformations of the two decamers.

*Temperature Dependence of the Aromatic Spectra.* The changes in chemical shifts of the aromatic protons with temperature have been used to determine the midpoint of the helix-to-coil transition ($T_m$) for a variety of nucleic acid oligomers. The limitations of this method have been recently discussed by Pardi et al. (1981). In particular, two assumptions must be made: (1) the system is in fast exchange throughout the transition and (2) the chemical shifts of the resonances in the single strands change linearly with temperature. The first assumption has been shown earlier not to be valid for the decamers studied here, at least below the $T_m$. The second assumption cannot be tested in self-complementary oligomers but has been shown to be invalid in non-self-complementary oligomers studied by Pardi et al. (1981). Nevertheless, approximate $T_m$'s can be obtained by examination of the shape of the chemical shift vs. temperature curve for various resonances in the molecule. Values obtained were 49–51 °C for the "GC" decamer and 50–53 °C for the "GC" decamer. Since the uncertainty is at least ±2 °C, it cannot be ascertained if the difference in the $T_m$'s for the two decamers is significant. The similar $T_m$'s obtained for the different base protons in each molecule indicate that the nonterminal base pairs melt cooperatively.

The chemical shifts of the nonexchangeable base protons were compared with results predicted from ring current shift calculations (Arter & Schmidt, 1971) (results not shown). Large discrepancies were noted between the calculated and experimental ring current shifts, and the general conclusion is that ring current shift calculations alone are unreliable for quantitative predictions of resonance positions (Kearns, 1977, 1983). Upfield shifts were observed for the "CG" GH8 resonance as well as the $T_2H6$ and $A_3H8$ proton in both decamers in going from helix to coil. The ring current shifts predicted for these protons in the double-stranded state are all small (<0.08 ppm) and upfield.

*Sugar Proton Coupling Constants and Conformation in the DNA Decamers.* Approximate coupling constants ($J_{1'2'} + J_{1'2'}$) for the H1′ sugars have been obtained indirectly by use of spin-echo experiments (Figure 12) as well as by direct measurement of the splittings in resolution-enhanced spectra (Figure 11). Values obtained were 14 ± 2 Hz. The H1′ sugar coupling can be related to the sugar conformation through the use of a modified Karplus equation (Altona & Sundaralingam, 1973; Haasnoot et al., 1981). Coupling constants ($J_{1'2'} + J_{1'2'}$) of ~9.7 Hz and ~16 Hz are predicted for the N-type (C2′-exo, C3′-endo) and S-type (C2′-endo, C3′-exo) sugar conformations, respectively. The observed values of coupling constants have been interpreted as a time-averaged blend of the two types (Davies, 1978). Predominantly S-type sugar pucker is expected for B-family DNA conformations. The results obtained here indicate ~65% S-type conformation for most sugars in both molecules, consistent with a B-DNA conformation, but not with either A- or Z-DNA conformations.

*Theoretical Analysis of Relaxation Rates.* Nonselective $T_1$ measurements on these and other DNA oligomers indicate that there is extensive spin diffusion even in relatively short DNAs (Kearns et al., 1981; Early et al., 1980). Therefore, in order to obtain meaningful information on structure, semiselective, selective, or biselective $T_1$ experiments and $T_2$ experiments must be done. The results of some experiments of this type have been presented in this paper. To facilitate analysis of the relaxation data obtained at 22 °C, we make the following assumptions.

*Assumption I.* The overall motion of the molecules in solution is isotropic and characterized by a single rotational correlation time, $\tau_c$, which is taken to be 6 ns at 20 °C. This assumption is justified by calculations for an ellipsoid of revolution with the same size as a DNA decamer (34 Å × 26 Å), and application of the Wöessner formula for relaxation in anisotropic molecules which indicates the error in using isotropic rotor behavior is negligible for this system. The use of a value of 6 ns for the effective rotational correlation is also reasonable since an isotropic rotor with a radius of 17 Å is calculated to have a 5-ns rotational correlation time at 22 °C (viscosity = 1 cP).

*Assumption II.* Internal motions are all assumed to have correlation times on the order of 0.5–1 ns with angular displacements of 20–30° consistent with previous $^1$H, $^{13}$C, and $^{31}$P NMR studies of DNA (Hogan & Jardetzky, 1980; Bolton & James, 1979; Levy et al., 1981; Rill et al., 1981; Shindo, 1981). Application of the Wöessner equations which include the effects of internal motions indicates that these internal motions will reduce the values of $R_1$ and $R_2$ calculated by using a rigid isotropic rotor model by ~35% and 50%, respectively.

*Assumption III.* The A·T and G·C base pairs are assumed to have the geometries indicated in Figure 1C. On the basis of our recent analysis of poly(dA-dT) (Kearns et al., 1981) and poly(dG-dC) (Mirau & Kearns, 1982), the N–H distance is assumed to be 1.15 Å in A·T and 1.05 Å in G·C base pairs.

With the above assumptions, the appropriate theoretical expressions for the proton–proton dipolar contributions to the selective spin–lattice relaxation rate [$R_1(s)$] and to the spin–spin relaxation rate ($R_2$) are (Abragam, 1978)

$$R_1^{H-H}(s) = f_1\frac{\gamma_H^4\hbar^2}{10r^6}\tau_c \qquad R_2^{H-H} = f_2\frac{\gamma_H^4\hbar^2}{4r^6}\tau_c \quad (1)$$

where $f_1 = 0.65$ and $f_2 = 0.5$ are the factors that take account of the effects of internal motion. We now use these equations to analyze the various relaxation rates which are summarized in Table VI.

*Imino Protons.* By use of the base pair geometry shown in Figure 1, the relaxation rates calculated by using a 6-ns correlation time generally agree well with those measured experimentally at 22 °C. For both the A·T and G·C base pairs a contribution of $\sim$0.9 $s^{-1}$ has been included to take into account the interaction of the imino protons with all other, more distant protons in the molecule. [This added contribution is based on coordinates for B-DNA (R. W. Behling, unpublished results), but its exact value is insensitive to the precise structure as it represents the sum of numerous small interactions.] As the base pair geometries are used as input in the calculations, we obtain no structural information from analysis of the low-field relaxation data. The main purpose of this aspect of the analysis is simply to demonstrate that the T and G imino proton relaxation rates can be accounted for by our model.

*AH2.* In the spin–spin relaxation experiment shown in Figure 12 we note that the two overlapping resonances assigned to $A_3H2$ and $A_9H2$ protons start with twice the intensity of the two other resolved AH2 resonances, but toward the end of the decay, they have the same magnitude as the single AH2 resonances. Even without any detailed analysis, this indicates that one (or both) of the pair of overlapping resonances has a larger relaxation rate than the other AH2 resonances, and this is seen quantitatively in the results given in Table V. The probable origin of this difference is suggested by the results of a recent study of relaxation in poly(dA-dT) (Assa-Munt et al., 1981; unpublished results), where we find evidence for a close approach between AH2 protons of adenine residues in *opposite* strands. The faster relaxation of the pair of $A_3H2$ and $A_9H2$ resonances is, therefore, attributed to a cross-strand AH2–AH2 interaction which is absent in the case of the $A_1H2$ and $A_7H2$ protons. Additional evidence for this interaction is found in the semiselective relaxation rate measurement where the rates for the AH2 protons of $A_{3,7,9}$ are found to be identical (0.65 $s^{-1}$) within experimental error (Table VI). The simultaneous polarization of two interacting protons eliminates their cross relaxation contribution to the initial value of $R_1$, and this accounts for the relatively slower spin–lattice relaxation rate (N. Assa-Munt et al., unpublished results; R. W. Behling, unpublished results). To account for the relaxation behavior of the two interacting AH2 protons, we find that an interpretation distance of 2.8 ± 0.2 Å is needed. This short distance requires propelling of the bases which we estimate to be >12°.

*GH8: Interactions with Sugar Protons.* Depending upon the precise model chosen for the DNA structure, the GH8 protons are expected to be close (within 1.9–2.5 Å) to the H2′ proton on the same nucleotide and to the H2″ proton of the 3′ nucleotide (i.e., 3′ $G_{5'}p_{3'}X$ 5′). The two-dimensional NMR results presented in the following paper (Feigon et al., 1983) clearly exhibit cross peaks due to these interactions between GH8 and sugar protons. The observed $R_1$ and $R_2$ values for the single GH8 resonance ($R_2 \sim 7$ $s^{-1}$) can be fit by a range of possible base–sugar proton distances including both sugar protons located at 2.2 Å or one within 2.0 Å and the other located at some distance on the order of 2.8 Å. The 2D-NMR experiments demonstrate that the stronger interaction is with a sugar proton in the same nucleotide (and therefore with the 2′ sugar proton).

*AH8.* The value of $R_2$ for the $A_7H8$ resonance ($R_2 = 10$ $s^{-1}$) is larger than for the GH8 resonance from the adjacent base pair ($R_2 \sim 7$ $s^{-1}$). While this could be due to differences in the AH8–sugar proton distances, interaction with the methyl group of adjacent thymine residue is the more likely explanation. The 2D-NMR data for d(ATATGCATAT) and d(ATATCGATAT) clearly demonstrate that the interactions with the 2′ and 2″ sugar protons are comparable for the GH8 and AH8 protons, whereas the AH8 protons exhibit a significant interaction with the thymine methyl protons of adjacent thymine residues. Under the assumption that the AH8 and GH8 interactions with the sugar protons are the same, the difference (3 $s^{-1}$) in the relaxation of the interior $A_7H8$ and $G_6H8$ resonances can be attributed to the AH8–TMe interaction. According to theory, an "effective" distance of 3.1 Å for each of the three methyl protons to AH8 would account for the estimated 3-$s^{-1}$ methyl contribution to the AH8 relaxation and explain why all of the AH8 protons in the two decamers (except for the terminal base pair) have faster relaxation rates than GH8, and why the TH6 relaxation ($R_2 \sim 14$ $s^{-1}$) is even faster, due to the strong interaction between TH6 and Me protons on the same residues.

*TH6.* The relaxation of the TH6 protons contains, in addition to contributions from sugar protons, a contribution from interactions with the three methyl protons. Because of the rapid rotation of the methyl group, we use an averaged interproton distance of 2.8 Å to account for the TH6–methyl interaction (Pegg et al., 1980), and this yields a contribution of 4 $s^{-1}$ to $R_2$. The net observed rate for the interior TH6 protons in both molecules is 14 ± 2 $s^{-1}$. If the sugar proton contributions to relaxation of the TH6 and AH8 protons are the same (i.e., 7 ± 2 $s^{-1}$) then we estimate that the methyl contributions to TH6 is (14 ± 2) − (7 ± 2) = 7±4 $sec^{-1}$ in agreement with the calculations. To test this point, selective and biselective relaxation rates for both the TH6 and methyl protons will have to be measured.

## Conclusions

In this paper various one-dimensional proton NMR experiments were used to study the two synthetic DNA decamers, d(ATATCGATAT) and d(ATATGCATAT). By use of the methods described in this paper, as well as the results of 2D-NOE experiments described in the following paper (Feigon et al., 1983), all of the base proton and imino proton resonances were assigned. The sugar conformations deduced from the coupling constants obtained were the same for both molecules and were consistent with B-family DNA, although close variants with similar sugar puckers are not eliminated. Spin–spin relaxation measurements showed no evidence for conformational differences between the two decamers, within the error of the experiment. The preliminary relaxation measurements are consistent with a B-family geometry in which base pairs are propelled (>12°). Both the imino and aromatic proton spectra were studied as a function of temperature. Although all of the imino proton resonances are broadened nearly to base line by 43 °C, a study of the base protons indicates that the $T_m$ for both of the decamers is $\sim$50 °C. Thus, care must be taken to distinguish between conformational changes associated with kinetic fraying or cracking of base pairs and thermodynamic melting of the helix to single

strands. The results of experiments described here lay the groundwork for further NMR studies on the interactions of drugs with these DNA decamers. Finally, we note that a very thorough one-dimensional NMR study of the self-complementary decanucleotide, d(CCAAGCTTGG), has been reported by Kan et al. (1982). They too were able to assign all of the base protons and the low-field imino resonances. In addition they have assigned the $H_1$ resonances and deduced sugar conformations from the splittings of the sugar resonances. No spin–lattice and spin–spin relaxation measurements were reported, however.

Acknowledgments

We thank R. W. Behling for preliminary relaxation data, computer calculations, and helpful discussions.

**Registry No.** d(ATATCGATAT), 83685-27-2; d(ATATGCATAT), 81065-64-7.

References

Abragam, A. (1978) *The Principles of Nuclear Magnetism*, The University Press, Oxford.
Altona, C., & Sundaralingam, M. (1973) *J. Am. Chem. Soc. 95*, 2333.
Arter, D. B., & Schmidt, P. G. (1976) *Nucleic Acids Res. 3*, 1437.
Assa-Munt, N., Granot, J., & Kearns, D. R. (1981) *Symp. Pap—Int. Biophys. Congr., 7th* (Abstracts).
Assa-Munt, N., Granot, J., Behling, R. W., & Kearns, D. R. (1984) *Biochemistry* (in press).
Behe, M., & Felsenfeld, G. (1981) *Proc. Natl. Acad. Sci. U.S.A. 78*, 1619.
Bendel, P., Laub, O., & James, T. L. (1982) *J. Am. Chem. Soc. 104*, 6748.
Bolton, P. H., & James, T. L. (1979) *J. Phys. Chem. 83*, 3359.
Borer, P. N., Dengler, B., Tinoco, I., Jr., & Uhlenbeck, O. C. (1974) *J. Mol. Biol. 86*, 843.
Borer, P. N., Kan, L. S., & Ts'o, P. O. P. (1975) *Biochemistry 14*, 4847.
Cheng, D. M., Kan, L.-S., Leutzinger, E. E., Jayaraman, K., Miller, P. S., & Ts'o, P. O. P. (1982) *Biochemistry 21*, 621.
Davies, D. B. (1978) *Prog. Nucl. Magn. Reson. Spectrosc. 12*, 135.
Denny, W. A., Cain, B. F., Atwell, G. J., Hansch, C., Panthananickal, A., & Leo, A. (1982a) *J. Med. Chem. 25*, 276.
Denny, W. A., Leupin, W., & Kearns, D. R. (1982b) *Helv. Chim. Acta 65*, 2372.
Drew, H., Takano, T., Tanaka, S., Itakura, K., & Dickerson, R. E. (1980) *Nature (London) 286*, 567.
Early, T. A., & Kearns, D. R. (1979) *Proc. Natl. Acad. Sci. U.S.A. 76*, 4165.
Early, T. A., Kearns, D. R., Burd, J. E., Larson, J. E., & Wells, R. D. (1977) *Biochemistry 16*, 541.
Early, T. A., Kearns, D. R., Hillen, W., & Wells, R. D. (1980) *Nucleic Acids Res. 8*, 5795.
Early, T. A., Kearns, D. R., Hillen, W., & Wells, R. D. (1981a) *Biochemistry 20*, 3756.
Early, T. A., Kearns, D. R., Hillen, W., & Wells, R. D. (1981b) *Biochemistry 20*, 3764.
Feigon, J. (1982) Ph.D. Thesis, University of California, San Diego.
Feigon, J., Wright, J. M., Denny, W. A., Leupin, W., & Kearns, D. R. (1982) *Cold Spring Harbor Symp. Quant. Biol. 47*, 207.
Feigon, J., Leupin, W., Denny, W. A., & Kearns, D. R. (1983) *Biochemistry* (following paper in this issue).
Freeman, R., & Hill, H. D. W. (1975) in *Dynamic Nuclear Magnetic Resonance Spectroscopy* (Jackman, L. M., & Cotton, F. A., Eds.) p 131, Academic Press, New York.
Granot, J., & Kearns, D. R. (1982) *Biopolymers 21*, 203.
Granot, J., Feigon, J., & Kearns, D. R. (1982) *Biopolymers 21*, 181.
Gutowsky, H. S., & Holm, C. H. (1956) *J. Chem. Phys. 25*, 1228.
Haasnoot, C. A. G., den Hartog, J. H. J., deRooij, J. F. M., van Boom, J. H., & Altona, C. (1980) *Nucleic Acids Res. 8*, 169.
Hahn, E. L., & Maxwell, D. E. (1952) *Phys. Rev. 88*, 1070.
Hilbers, C. W., & Patel, D. J. (1975) *Biochemistry 14*, 2456.
Hogan, M. E., & Jardetzky, O. (1980) *Biochemistry 19*, 3460.
Johnston, P. D., & Redfield, A. G. (1977) *Nucleic Acids Res. 4*, 3599.
Kallenbach, N. R., Daniel, W. E., Jr., & Kaminder, M. A. (1976) *Biochemistry 6*, 1218.
Kan, L.-S., Borer, P. N., & Ts'o, P. O. P. (1975) *Biochemistry 14*, 4864.
Kan, L.-S., Cheng, D. M., Jayaraman, K., Leutzinger, E. E., Miller, P. S., & Ts'o, P. O. P. (1982) *Biochemistry 21*, 6723.
Kearns, D. R. (1977) *Annu. Rev. Biophys. Bioeng. 6*, 477.
Kearns, D. R. (1983) *CRC Crit. Rev. Biochem.* (in press).
Kearns, D. R., Assa-Munt, N., Behling, R. W., Early, T. A., Feigon, J., Granot, J., Hillen, W., & Wells, R. D. (1981) in *Biomolecular Stereodynamics* (Sarma, R. H., Ed.) Vol. I, pp 345–366, Adenine Press, New York.
Klysik, J., Stirdivant, S. M., Larson, J. E., Hart, P. A., & Well, R. D. (1981) *Nature (London) 290*, 672.
Levy, G. D., Hilliard, P. R., Jr., Levy, L. F., & Rill, R. L. (1981) *J. Biol. Chem. 256*, 9986.
Malfoy, B., Rousseau, N., & Leng, M. (1982) *Biochemistry 21*, 5463.
Mirau, P. A., & Kearns, D. R. (1983) in *Structure and Dynamics: Nucleic Acids and Proteins* (Clementi, E., & Sarma, R. H., Eds.) pp 227–239, Adenine Press, New York.
Pardi, A., & Tinoco, I., Jr. (1982) *Biochemistry 21*, 4686.
Pardi, A., Martin, F. H., & Tinoco, I., Jr. (1981) *Biochemistry 20*, 3986.
Patel, D. J. (1975) *Biochemistry 14*, 3984.
Patel, D. J. (1976) *Biopolymers 15*, 533.
Patel, D. J., & Hilbers, C. W. (1975) *Biochemistry 14*, 2651.
Patel, D. J., & Tonelli, A. E. (1975) *Biochemistry 14*, 3990.
Patel, D. J., & Canuel, L. L. (1976a) *Proc. Natl. Acad. Sci. U.S.A. 73*, 674.
Patel, D. J., & Canuel, L. L. (1976b) *Proc. Natl. Acad. Sci. U.S.A. 73*, 3343.
Patel, D. J., & Canuel, L. L. (1977a) *Biopolymers 16*, 857.
Patel, D. J., & Canuel, L. L. (1977b) *Proc. Natl. Acad. Sci. U.S.A. 74*, 5207.
Patel, D. J., Kozlowski, S. A., Marky, L. A., Broka, C., Rice, J. A., Itakura, K., & Breslauer, K. J. (1982a) *Biochemistry 21*, 428.
Patel, D. J., Kozlowski, S. A., Marky, L. A., Rice, J. A., Broka, C., Dallas, J., Itakura, K., & Breslauer, K. J. (1982b) *Biochemistry 21*, 437.
Patel, D. J., Kozlowski, S. A., Marky, L. A., Rice, J. A., Broka, C., Itakura, K., & Breslauer, K. J. (1982c) *Biochemistry 21*, 451.
Patel, D. J., Kozlowski, S. A., Marky, L. A., Rice, J. A., Broka, C., Itakura, K., & Breslauer, K. J. (1982d) *Biochemistry 21*, 445.
Peck, L. J., Nordheim, A., Rich, A., & Wang, J. C. (1982) *Proc. Natl. Acad. Sci. U.S.A. 79*, 4560.

Pegg, D. T., Bendall, M. R., & Doddrell, D. M. (1980) *Aust. J. Chem. 33*, 1167.
Ramstein, J., & Leng, M. (1980) *Nature (London) 288*, 413.
Redfield, A. G., Roy, S., Sanchez, V., Tropp, J., & Figueroa, N. (1981) in *Biomolecular Stereodynamics Conference* (Sarma, R., Ed.) p 195, Academic Press, New York.
Rill, R. L., Hilliard, P. R., Jr., Levy, L. F., & Levy, G. C. (1981) in *Biomolecular Stereodynamics* (Sarma, R. H., Ed.) Vol. I, p 383, Adenine Press, New York.
Romaniuk, P. J., Hughes, D. W., Gregoire, R. J., Neilson, T., & Bell, R. A. (1978) *J. Am. Chem. Soc. 100*, 3971.
Sanchez, V., Redfield, A. G., Johnston, P. D., & Tropp, J. (1980) *Proc. Natl. Acad. Sci. U.S.A. 77*, 5659.
Schweizer, M. P., Chan, S. I., Helmkamp, G. K., & Ts'o, P. O. P. (1964) *J. Am. Chem. Soc. 86*, 696.
Shindo, H. (1981) *Eur. J. Biochem. 120*, 309.
Taylor, R., & Kennard, O. (1982) *J. Am. Chem. Soc. 104*, 3209.
Ts'o, P. O. P., Barrett, J. C., Kan, L. S., & Miller, P. S. (1973) *Ann. N.Y. Acad. Sci. 222*, 290.
Wang, A. H.-J., Quigley, G. J., Kolpak, F. J., Crawford, J. L., van Boom, J. H., van der Marel, G., & Rich, A. (1979) *Nature (London) 282*, 680.
Wartell, R. M., Klysik, J., Hillen, W., & Wells, R. D. (1982) *Proc. Natl. Acad. Sci. U.S.A. 79*, 2549.
Wöessner, D. E. (1962) *J. Chem. Phys. 37*, 647.
Wood, D. J., Hruska, F. E., & Ogilive, K. K. (1974) *Can. J. Chem. 52*, 3353.
Wright, J. M., Feigon, J., Denny, W. A., Leupin, W., & Kearns, D. R. (1981) *J. Magn. Reson. 45*, 514.